Tribocorrosion behavior of electroless Ni-P/Ni-B duplex coating on AA7075 aluminum alloy

Harun Mindivan
Department of Mechanical Engineering, Bilecik Şeyh Edebali University, Bilecik, Turkey

Abstract

Purpose – This paper aims to investigate the structural, corrosion and the study of tribocorrosion features of the AA7075 aluminum alloy with and without the application of electroless Ni-P/Ni-B duplex coating with a thickness of approximately 40 microns.

Design/methodology/approach – Surface characterization of the samples was made by structural surveys (light optic microscope, scanning electron microscopic examinations and X-ray diffraction analyses), hardness measurements, corrosion and tribocorrosion tests.

Findings – Results of the experiments showed that upper Ni-B coating deposited on the surface of first Ni-P layer by duplex treatment caused remarkable increment in the hardness, corrosion resistance and tribocorrosion performance as compared to the AA7075 aluminum alloy.

Originality/value – This study can be a practical reference and offers insight into the effects of duplex treating on the increase of hardness, corrosion and tribocorrosion performance.

Keywords Tribocorrosion, Corrosion, Electroless Ni-P/Ni-B duplex coating, AA7075 aluminum alloy

Paper type Research paper

1. Introduction

Aluminum alloys are widely used as structural materials in the component design because of their excellent properties as high strength to weight ratio, high electrical and thermal conductivities and good formability. According to the literature, however, their low hardness and poor tribological properties (high friction coefficient, serious wear and a tendency for cold-welding when mated with other metals) are the bottleneck of unprotected aluminum alloys (Saglam *et al.*, 2004; Mindivan *et al.*, 2005). On the other hand, thin porous natural oxide on surface of aluminum in corroding environment might be formed which causes localization of corrosion reactions in these sites (Saglam *et al.*, 2004). For some parts in which a superior wear resistance at demanding conditions is required, surface-engineered aluminum components could be able to withstand in corrosive conditions while simultaneously offering an improved wear protection. Among the surface engineering techniques used to protect aluminum alloys, electroless deposition appeared as a popular surface treatment technique generating an enriched layer that can improve the practical usage of aluminum and its alloys (Sudagar *et al.*, 2010; Vitry *et al.*, 2012; Vijayanand and Elansezhian, 2014; Subramanian and Palaniradja, 2015; Yildiz *et al.*, 2017).

A solution that could provide better corrosion and wear protection is the electroless deposition of Ni-P/Ni-B duplex coating on aluminum components with complex shapes because of its excellent properties such as high hardness, good wear and corrosion resistances and uniform thickness (Yildiz *et al.*, 2017; Mindivan and Mindivan, 2017). In this way, it is possible to couple the light weight and relatively low-cost nature of aluminum with the high superficial properties of electroless Ni-P/Ni-B duplex coating. As an electroless Ni-P as the internal layer had gained immense popularity before plating aluminum with electroless Ni-B (Vitry *et al.*, 2012; Subramanian and Palaniradja, 2015), a duplex coating deposited on AA7075 aluminum alloy by sequential immersion in two different electroless plating baths was prepared. In this work on duplex Ni-P/Ni-B coating on AA7075 aluminum alloy, the effectiveness of this coating system in improving the corrosion and tribocorrosion behavior of light weight and high-strength aluminum alloy was demonstrated.

2. Experimental details

AA7075 grade aluminum disks (with 25 mm of diameter) were used as substrate for the deposition of Ni-P/Ni-B films. This grade was chosen because it is a good candidate material for aerospace applications. The substrates were prepared for plating by mechanical grinding and polishing, alkaline cleaning, pickling and pretreatment procedures (Mindivan, 2016). The duplex coating was prepared by sequential immersion in the two respective plating baths for 120 mins to gain similar thickness of individual Ni-P and Ni-B layers. A thin (approximately 20 μm) but continuous Ni-P (Durni-Coat DNC 520-9) underlayer was applied before immersion in the electroless Ni-B bath, to serve as a catalyst for initial Ni-B deposition. After coating of the first layer (Ni-P) (Mindivan, 2016), the Ni-P coated sample was made to react in Ni-B bath for the deposition of boron which is acting as second layer. The actual plating took place at 95 ± 1°C in a thermostable cell with a volume of 250 ml, under constant mechanical agitation.

The current issue and full text archive of this journal is available on Emerald Insight at: **www.emeraldinsight.com/0036-8792.htm**

Industrial Lubrication and Tribology
71/5 (2019) 630–635

[DOI 10.1108/ILT-05-2018-0177]

Received 5 May 2018
Revised 5 May 2018
Accepted 22 May 2018

Industrial Lubrication and Tribology
Volume 71 · Number 5 · 2019 · 630–635

Here, the pH of 14 was maintained for better deposition of Ni-B. The electroless Ni-B deposition was carried out using sodium borohydride ($NaBH_4$) as a reducer, nickel chloride hexahydrate ($NiCl_2.6H_2O$) as a nickel source, ethylenediamine ($NH_2–CH_2–CH_2–NH_2$) as a complexing agent and lead nitrate ($PbNO_3$) as a stabilizer. Detail procedure of the plating process has been described extensively elsewhere (Mindivan and Mindivan, 2017).

Microstructural characterization was made by microscopic examinations, X-ray diffraction (XRD) and microhardness measurements. The surface morphology and cross-section of the coating were studied by a Zeiss Supra field emission gun scanning electron microscope (FEG-SEM) equipped with the energy dispersive X-ray (EDX) spectroscopy and a Nikon Eclipse LV150 Light Optic Microscope (LOM), respectively. XRD analysis was carried out by using CuKα radiation with a panalytical empyrean diffractometer. Knoop indentation on polished cross-sections was used to obtain hardness values that are completely uninfluenced by the substrate hardness. The corresponding final values were reported as the average of five measurements.

The electrochemical tests were carried out using a Gamry model PC4/300 mA potentiostat/galvanostat controlled by a computer with DC 105 Corrosion analysis software in the corroding media of aerated solution of 3.5 Wt.% NaCl at room temperature. Before potentiodynamic polarization measurements, a stabilization period of 45 min was used to measure the open circuit potential (OCP) between working and reference electrodes. Potentiodynamic polarization curves were generated by sweeping the potential from cathodic to anodic direction at a scan rate of 1 mVs^{-1}, starting from −1 up to +1 V. The corrosion tests were evaluated from the potentiodynamic polarization. Finally, the surface images of the corroded samples were examined using FEG-SEM to determine the morphology of the developed corrosion.

The tribocorrosion tests of the polished AA7075 aluminum substrate and Ni-P/Ni-B-coated sample were conducted in a triboelectrochemical cell containing 25 ml of 3.5 Wt.% NaCl solution by using a ball-on-disk reciprocating tribometer coupled with a three electrode electrochemical cell. Reciprocating sliding wear tests were performed in a reciprocating mode with a 1.7 cm s^{-1} sliding rate under 5 N applied load for 45 min at OCP conditions. The OCP was measured before, during and after sliding where the sliding action started after reaching the stable OCP values for each test. The counter body was an Al_2O_3 ball with 10 mm diameter. The choice of Al_2O_3 ball as the counter body was made because of its high hardness, high wear resistance, chemical inertness and electrical insulating properties. The ball holder was made of a polymeric material to prevent the corrosion effects. During the test, surface with an area of 1.2 cm^2 was exposed to the corrosive electrolyte. All tribocorrosion tests were repeated at least two times to have repeatability. After tribocorrosion tests, the worn surfaces of the wear tracks that formed on the examined samples were investigated by the FEG-SEM.

3. Results and discussions

Figure 1 depicts surface morphology and cross-sectional micrograph of the Ni-P/Ni-B duplex-coated sample. For each

Figure 1 (a) Surface morphology and (b) cross-section LOM image of the Ni-P/Ni-B duplex-coated sample

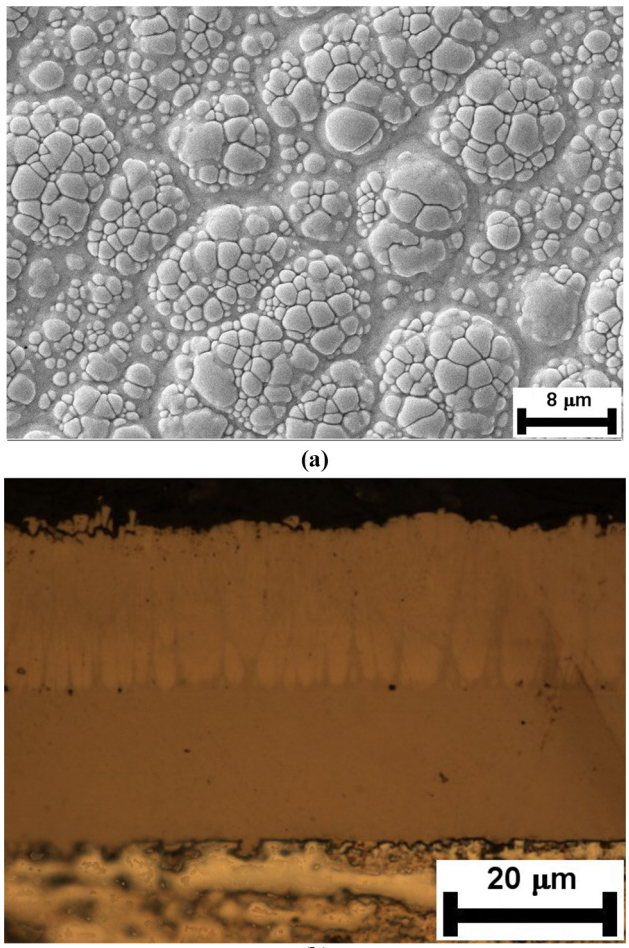

layer coating, the plating thickness of Ni-P and Ni-B layer in the duplex coating was approximately 20 μm, as shown in Figure 1(b). It can be seen that the Ni-P/Ni-B duplex-coated sample exhibited a dense structure with good adhesion to the substrate and a strong bonding was achieved between the two layers. In general, the Ni-B coating was rather compact without macro-defects such as porosity and presented the typical cauliflower like texture [Figure 1(a)]. In the case of duplex-coated sample [Figure 1(b)], the two layers kept their typical features. However, the interface obtained when Ni-P constituted the first layer [Figure 1(b)]was totally planar, while the obtained Ni-B coating was slightly wavy due to the columnar growth in that coating. To find out the composition of the duplex coating, EDX analysis has been carried out and the obtained results are given in Table I. From the Table I, it is evident that the first Ni-P coating deposited on the AA7075 aluminum alloy contained about 11.6 Wt.% P, while the Ni-B deposit with 4.0 Wt.% B content appeared to reflect the amorphous structure of the coating. The diffraction pattern of the Ni-P/Ni-B duplex-coated sample shown in Figure 2 was a single broad peak in diffraction angle between 35 and 55° that indicated the presence of amorphous nature in the coating. The

Table I Chemical composition of the electroless coating

Types of coating	Ni (Wt.%)	P (Wt.%)	B (Wt.%)
Ni-P	88.3	11.6	–
Ni-B	96.0	–	4.0

Figure 2 XRD pattern for the Ni-P/Ni-B duplex-coated sample

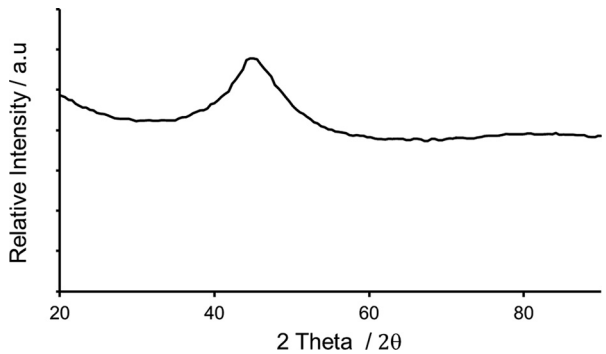

XRD result corroborated well with the boron content observed in the EDX result.

Figure 3 shows the Knoop indentations across the Ni-P/Ni-B duplex-coated sample and Knoop hardness plot along the polished cross-section of the Ni-P/Ni-B duplex-coated sample. The hardness values measured under an applied load of 0.1 N decreased gradually from the outermost surface layer to the inner regions of the duplex-coated sample [Figure 3(b)]. The hardness of the Ni-B layer itself was about 835 $HK_{0.01}$ which corresponded to the hardness of ferrous cutting tools. This extremely high hardness value can be attributed to the internal stress that is saved in the layers (Tohidi *et al.*, 2017). Although the thickness of Ni-B top layer was almost 20 μm [Figure 3(a)], base metal hardness value (78.5 $HK_{0.01}$) was reached at about 50 μm away from the outer surface due to the compressive stress of the Ni-P sub-layer with high phosphorus content.

In the present study, the Ni-P/Ni-B duplex-coated sample showed relatively good resistance to corrosion in 3.5 Wt.% NaCl solution as witnessed from Figure 4. The application of Ni-P layer before the Ni-B electroless layer can improve the surface resistance by serving as a protective layer that acts as a barrier against the diffusion of corrosive ions to the bare substrate. Mafi and Dehghanian (2011) have reported that amorphous Ni-P coatings with high phosphorus content have very high corrosion resistance. Both the high phosphorus content (11.6 Wt.%) in the Ni-P sub-layer (Rezagholizadeh *et al.*, 2015; Panja *et al.*, 2016) and the dense and compact structure of the Ni-B top layer (Wan *et al.*, 2016) shifted the corrosion potential, E_{corr}, to the upwards and decreased the corrosion current density, I_{corr}, and consequently improved the corrosion resistance. The corrosion potential of the Ni-P/Ni-B duplex-coated sample shifted to more positive potential value (−725 mV) and lower current density value (1.69×10^{-6} A/cm^2) than those of the untreated AA7075 aluminum alloy (−1050 mV and 51.8×10^{-6} A/cm^2). The corrosion morphologies of untreated AA7075 aluminum alloy and

Figure 3 (a) Knoop indentations across the Ni-P/Ni-B duplex-coated sample and (b) cross-section hardness profile of the Ni-P/Ni-B duplex-coated sample

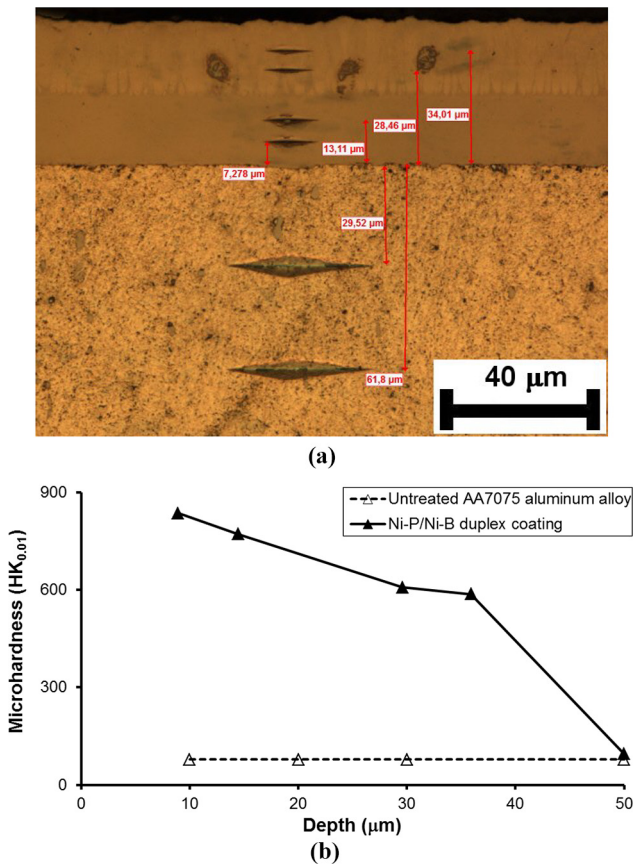

Figure 4 Potentiodinamic polarization curves of the untreated AA7075 aluminum alloy and Ni-P/Ni-B duplex-coated sample in 3.5 Wt.% NaCl solution

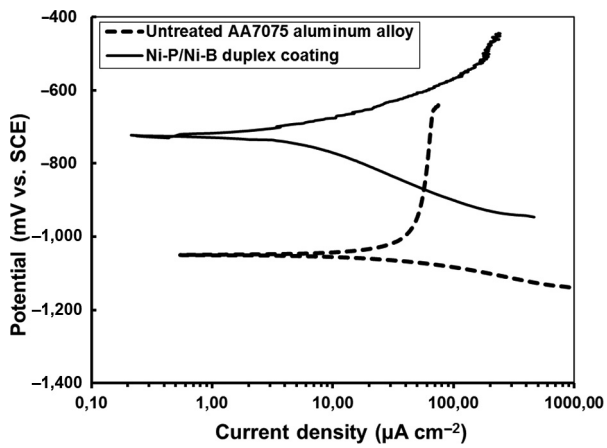

Ni-P/Ni-B duplex-coated sample after polarization tests can be seen in Figure 5. No pitting was observed on the surface of the electroless Ni-P/Ni-B duplex-coated sample. In contrast, many pittings can be seen on the untreated AA7075 aluminum alloy

Figure 5 FEG-SEM surface morphologies after polarization tests of the (a) untreated AA7075 aluminum alloy and (b) Ni-P/Ni-B duplex-coated sample (low and high magnifications)

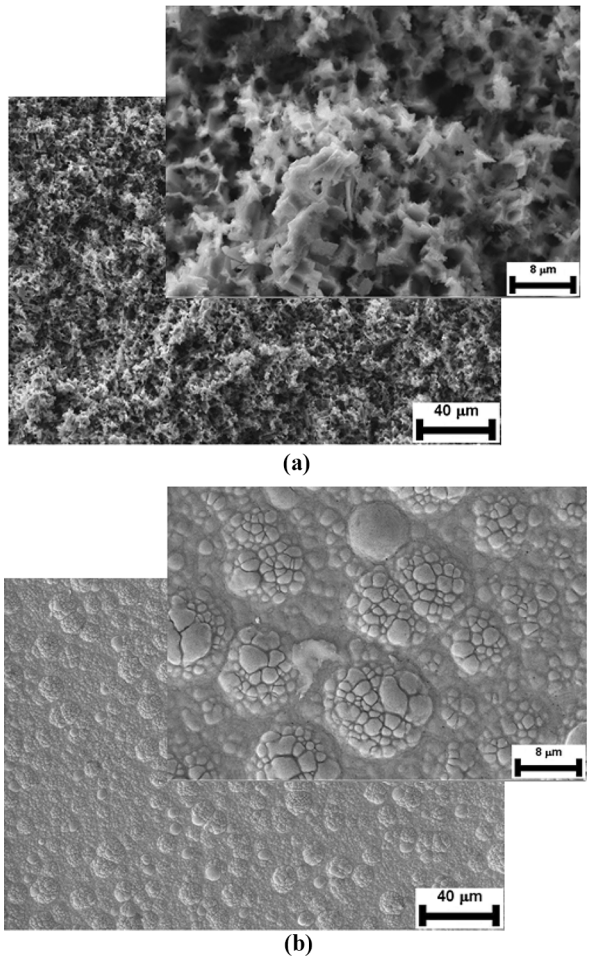

Figure 6 Evolution of the (a) OCP and (b) friction coefficient during the OCP tribocorrosion tests

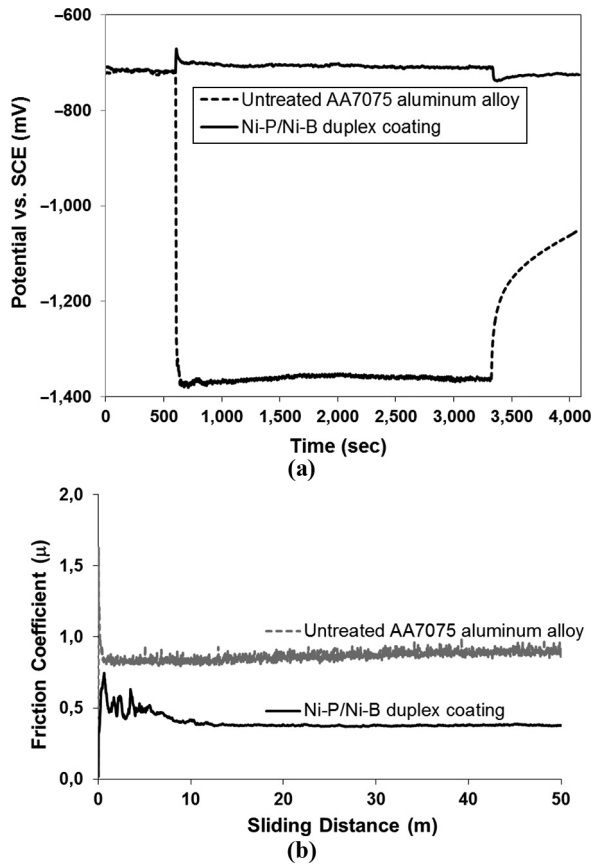

surface. These results are in agreement with the results of the polarization measurement.

The tribocorrosion tests were performed at OCP conditions, and the evolution of the potential as a function of time is shown in Figure 6(a) along with their corresponding friction curves with respect to sliding distance in Figure 6(b). The change in OCP of the untreated 7075 aluminum substrate and Ni-P/Ni-B duplex-coated sample was measured before the onset of sliding, during sliding and after the sliding motion was stopped. Before the onset of sliding, the OCP of the untreated AA7075 aluminum substrate was −730 mV, while for the duplex-coated sample; the OCP was −715 mV. When sliding started, it can be clearly seen that the duplex-coated sample exhibited a totally different behavior, where the OCP values increased. This indicates that the duplex-coated sample was not destroyed during sliding under this testing condition. In fact, the cross-section scans performed across each wear showed that the depth of the wear track for the duplex-coated sample was measured as 1.5 ± 0.01 μm [Figure 7(b)]. It should be noted that the depth of the wear track formed on the duplex-coated sample (approximately 1.5 μm) was well below the thickness of the Ni-B layer (approximately 20 μm). Therefore, the underlying Ni-P layer was neither exposed to the corrosive environment nor affected by plastic deformation along the sliding direction. The absence of drop in the duplex-coated sample can be attributed to the increased wear resistance given by the Ni-B layer. On the other hand, in case of the untreated AA7075 aluminum alloy, when sliding started, a sudden drop in the potential of approximately 640 mV can be observed. The OCP drop indicated a partial removal of the passive film by the mechanical action (Mindivan and Mindivan, 2016; Mindivan *et al.*, 2017) suggesting an increase in susceptibility of the nascent active AA7075 aluminum alloy for corrosion, and therefore a need for surface protection. In this case, the depth of the wear track for the untreated AA7075 aluminum alloy was found to be approximately 55 ± 0.6 μm [Figure 7(a)]. It should be noted that the OCP stayed low during the rubbing action of Al_2O_3 ball, constant at approximately −1370 mV (Mindivan and Mindivan, 2016; Mindivan *et al.*, 2017; Fernandes *et al.*, 2006; Azzia *et al.*, 2009). When the sliding motion was stopped, the potential of untreated AA7075 aluminum substrate exhibited a shift in the noble direction with respect to the OCP, suggesting a progressive repassivation of the wear track area. Besides, the corresponding high friction coefficient fluctuations [Figure 6(b)] for the untreated AA7075 aluminum substrate provide supplemental evidence for the

Figure 7 The 3D profiles of the wear tracks formed on the surfaces of the (a) untreated AA7075 aluminum substrate and (b) Ni-P/Ni-B duplex-coated sample

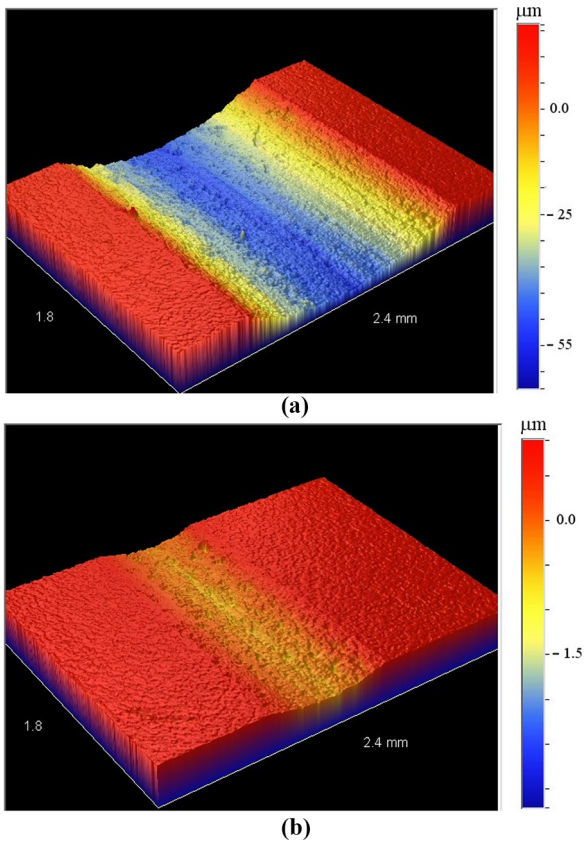

Figure 8 Worn surface FEG-SEM micrographs of the (a) untreated AA7075 aluminum alloy and (b) Ni-P/Ni-B duplex-coated sample against Al_2O_3 balls (low and high magnifications)

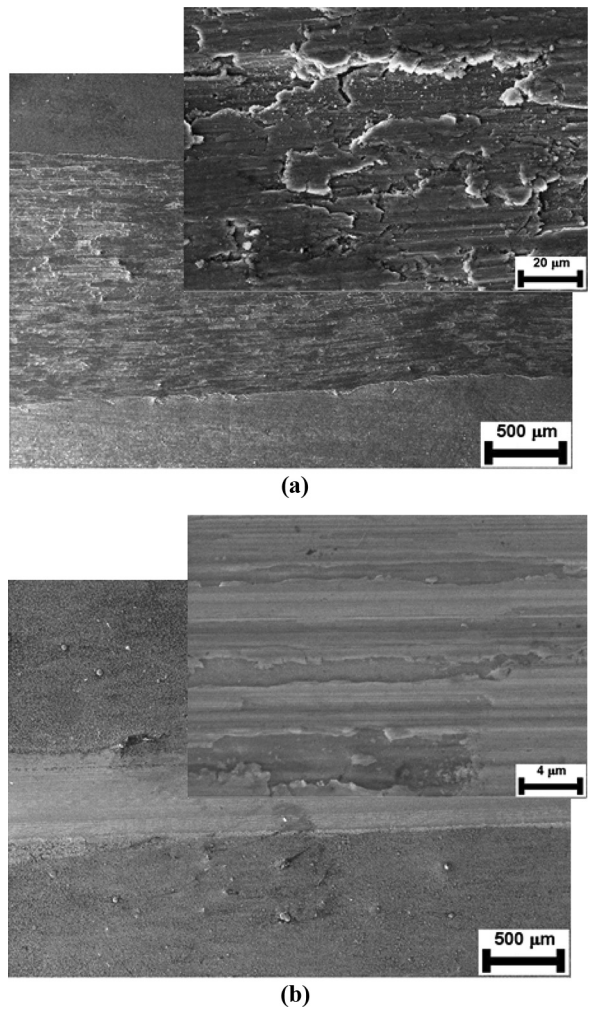

OCP variations obtained in this study. The untreated AA7075 aluminum substrate exhibited the highest and most unstable friction coefficient (0.86 ± 0.08). Such large fluctuations in the friction coefficient have been attributed to the formation of third body particles during wear testing (Mindivan *et al.*, 2009). On the other hand, it can be clearly seen that the duplex-coated sample showed a lower and more stable friction coefficient (0.39 ± 0.03) when compared with the untreated AA7075 aluminum substrate. The cauliflower like structures make the deposits naturally lubricious (Subramanian and Palaniradja, 2015; Mindivan and Mindivan, 2017). A typical columnar morphology can be seen in the cross-sectional micrograph due to the growth mechanism of the columns reducing the actual contact area [Figure 1(b)]. These columnar structures act as the friction-reducing performance in aqueous environment (Wan *et al.*, 2016).

Figure 8 presents FEG-SEM micrographs of the worn surfaces of the untreated AA7075 aluminum substrate and Ni-P/Ni-B duplex-coated sample. The untreated AA7075 aluminum substrate showed severe damages due to the mechanical action of the hard Al_2O_3 ball, whereas the Ni-P/Ni-B duplex-coated sample was less affected; this was clearly revealed by the low and high magnification FEG-SEM micrographs. It is concluded that the hard Ni-B top layer deposited on the Ni-P sub-layer with high phosphorus content noticeably improved the tribocorrosion performance of the untreated AA7075 aluminum substrate.

4. Conclusions

In this study, the structural features, corrosion and tribocorrosion behavior of Ni-P/Ni-B duplex coating deposited on AA7075 aluminum alloy substrate were investigated. The result showed the following:

- Application of the Ni-B layer as an outermost layer after the Ni-P electroless layer produced a continuous nodular surface layer with a columnar cross-section. This top layer exhibited extremely high hardness value (835 $HK_{0.01}$) as compared to the base metal (78.5 $HK_{0.01}$).
- Tribocorrosion tests revealed that, upper Ni-B coating deposited on the surface of first Ni-P layer by duplex treatment caused a further increase in the corrosion resistance and tribocorrosion performance along with a significant reduction in the friction coefficient when compared to the untreated AA7075 aluminum alloy.

References

Azzia, M., Paquette, M., Szpunar, J.A., Klemberg-Sapieha, J. E. and Martinu, L. (2009), "Tribocorrosion behaviour of DLC-coated 316L stainless steel", *Wear*, Vol. 267 Nos 5/8, pp. 860-866.

Fernandes, A.C., Vaz, F., Ariza, E., Rocha, L.A., Ribeiro, A.R. L., Vieira, A.C., Rivière, J.P. and Pichon, L. (2006), "Tribocorrosion behaviour of plasma nitrided and plasma nitrided + oxidised Ti6Al4V alloy", *Surface & Coatings Technology*, Vol. 200, pp. 6218-6224.

Mafi, I.R. and Dehghanian, C. (2011), "Comparison of the coating properties and corrosion rates in electroless Ni–P/PTFE composites prepared by different types of surfactants", *Applied Surface Science*, Vol. 257 No. 20, pp. 8653-8658.

Mindivan, H. (2016), "Wear and corrosion resistance of Ni-P coating on AA7075 aluminum alloy", *Machines, Technologies, Materials*, Vol. 6, pp. 29-31.

Mindivan, F. and Mindivan, H. (2016), "Surface properties and tribocorrosion behaviour of a thermal sprayed martensitic stainless steel coating after pulsed plasma nitriding process", *Journal Advances in Materials and Processing Technologies*, Vol. 2 No. 4, pp. 514-526.

Mindivan, F. and Mindivan, H. (2017), "The study of electroless Ni-P/Ni-B duplex coating on HVOF-sprayed martensitic stainless steel coating", *Acta Physica Polonica A*, Vol. 131 No. 1, pp. 64-67.

Mindivan, F., Mindivan, H. and Darcan, C. (2017), "Electroless Ni–B coating of pure titanium surface for enhanced tribocorrosion performance in artificial saliva and antibacterial activity", *Tribology in Industry*, Vol. 39 No. 2, pp. 270-276.

Mindivan, H., Baydogan, M., Kayalı, E.S. and Cimenoglu, H. (2005), "Wear behaviour of 7039 aluminum alloy", *Materials Characterization*, Vol. 54 No. 3, pp. 263-269.

Mindivan, H., Tekmen, C., Dikici, B., Tsunekawa, Y. and Gavgali, M. (2009), "Wear behavior of plasma sprayed composite coatings with in situ formed Al_2O_3", *Materials & Design*, Vol. 30, pp. 4516-4520.

Panja, B., Das, S.K. and Sahoo, P. (2016), "Tribological behavior of electroless Ni–P coatings in various corrosive environments", *Surface Review and Letters*, Vol. 23 No. 5, pp. 1-18.

Rezagholizadeh, M., Ghaderi, M., Heidary, A. and Vaghefi, S. M.M. (2015), "Electroless Ni–P/Ni–B–B_4C duplex composite coatings for improving the corrosion and tribological behavior of Ck45 steel", *Protection of Metals and Physical Chemistry of Surfaces*, Vol. 51 No. 2, pp. 234-239.

Saglam, U., Baydogan, M., Mindivan, H., Kayalı, E.S. and Cimenoglu, H. (2004), "Influence of retrogression and reageing on mechanical and corrosion properties of 7039 aluminium alloy", *Zeitschrift Für Metallkunde*, Vol. 95, pp. 14-17.

Subramanian, C. and Palaniradja, K. (2015), "Effect of surfactant on the electroless Ni-P/Ni-B duplex coatings on aluminium 7075", *International Journal of Metallurgical Engineering*, Vol. 4 No. 2, pp. 25-32.

Sudagar, J., Venkateswarlu, K. and Lian, J. (2010), "Dry sliding wear properties of a 7075-T6 aluminum alloy coated with Ni-P (h) in different pretreatment conditions", *Journal of Materials Engineering and Performance*, Vol. 19 No. 6, pp. 810-818.

Tohidi, A., Monirvaghefi, S.M. and Hadipour, A. (2017), "Properties of electroless Ni–B and Ni–P/Ni–B coatings formed on stainless steel", *Transactions of the Indian Institute of Metals*, Vol. 70 No. 7, pp. 1735-1742.

Vijayanand, M. and Elansezhian, R. (2014), "Effect of different pretreatments and heat treatment on wear properties of electroless Ni-B coatings on 7075-T6 aluminum alloy", *Procedia Engineering*, Vol. 97, pp. 1707-1717.

Vitry, V., Sens, A., Kanta, A.F. and Delaunois, F. (2012), "Wear and corrosion resistance of heat treated and as-plated duplex NiP/NiB coatings on 2024 aluminum alloys", *Surface & Coatings Technology*, Vol. 206, pp. 3421-3427.

Wan, Y., Yu, Y., Cao, L., Zhang, M., Gao, J. and Qi, C. (2016), "Corrosion and tribological performance of PTFE-coated electroless nickel boron coatings", *Surface & Coatings Technology*, Vol. 307, pp. 316-323.

Yildiz, R.A., Genel, K. and Gulmez, T. (2017), "Effect of heat treatments for electroless deposited Ni-B and Ni-W-B coatings on 7075 Al alloy", *International Journal of Materials, Mechanics and Manufacturing*, Vol. 5 No. 2, pp. 83-86.

Corresponding author

Harun Mindivan can be contacted at: hmindivan@hotmail.com